Sideband cooling of ions in a non-neutral buffer gas

A. Kellerbauer,[1,*] M. Amoretti,[2,3] G. Bonomi,[1] P. D. Bowe,[4] C. Canali,[2,3] C. Carraro,[2,3] C. L. Cesar,[5] M. Charlton,[4] M. Doser,[1] A. Fontana,[6,7] M. C. Fujiwara,[8] R. Funakoshi,[9] P. Genova,[6,7] R. S. Hayano,[9] I. Johnson,[10] L. V. Jørgensen,[4] V. Lagomarsino,[2,3] R. Landua,[1] E. Lodi Rizzini,[11,7] M. Macrí,[2,3] N. Madsen,[12] D. Mitchard,[4] P. Montagna,[6,7] L. G. C. Posada,[9] A. Rotondi,[6,7] G. Testera,[2,3] A. Variola,[4] L. Venturelli,[11,7] D. P. van der Werf,[4] Y. Yamazaki,[8] and N. Zurlo[11,7]

(ATHENA Collaboration)

[1]*Department of Physics, CERN, 1211 Genève 23, Switzerland*

[2]*Dipartimento di Fisica, University of Genoa, 16146 Genova, Italy*

[3]*INFN Sezione di Genova, 16146 Genova, Italy*

[4]*Department of Physics, University of Wales Swansea, Swansea SA2 8PP, United Kingdom*

[5]*Instituto di Fisica, Federal University of Rio de Janeiro, Rio de Janeiro 21945-970, Brazil*

[6]*Dipartimento di Fisica Nucleare e Teorica, University of Pavia, 27100 Pavia, Italy*

[7]*INFN Sezione di Pavia, 27100 Pavia, Italy*

[8]*Atomic Physics Laboratory, RIKEN, Saitama 351-0198, Japan*

[9]*Department of Physics, University of Tokyo, Tokyo 113-0033, Japan*

[10]*Physik-Institut, University of Zürich, 8057 Zürich, Switzerland*

[11]*Dipartimento di Chimica e Fisica per l'Ingegneria e per i Materiali, University of Brescia, 25123 Brescia, Italy*

[12]*Department of Physics and Astronomy, University of Aarhus, 8000 Aarhus C, Denmark*

(Received 11 November 2005; published 19 June 2006)

We have investigated an extension of the buffer gas cooling technique to a non-neutral buffer gas. The proposed scheme will allow efficient mass-selective centering of ions confined in a Penning trap in situations where the use of a neutral damping agent is not possible. The present paper reviews the principle of the technique and reports on evidence for sideband cooling of antiprotons in an electron gas, obtained with the ATHENA apparatus at CERN's Antiproton Decelerator facility.

DOI: 10.1103/PhysRevA.73.062508 PACS number(s): 36.10.−k, 52.20.Hv, 52.27.Jt

I. INTRODUCTION

The studies of ground-state properties of elementary particles, of exotic atoms, and of antimatter bound states all rely on long observation times, which can be achieved by confinement in a trap. The prominent tool for the confinement of charged particles over macroscopic times is the Penning trap, which combines radial confinement by a strong axial solenoidal magnetic field with a three-dimensional quadrupolar electric field for axial confinement. The motion of single ions [22] in a Penning trap has been fully described both classically and quantum mechanically [1].

ATHENA is an experiment installed at the CERN Antiproton Decelerator (AD) [2] whose goal is the production and detection of copious amounts of cold antihydrogen ($\bar{H}$) atoms. The centerpiece of the ATHENA apparatus is a long cylindrical electromagnetic trap whose electrostatic potentials can be freely set to form one or several Penning traps for particle capture, cooling, and manipulation. Ultimately, the produced cold anti-atoms are intended to be used for a test of CPT/Lorentz symmetry by comparing their atomic spectrum with that of their ordinary-matter counterparts as well as for a first-ever test of gravitational attraction on antimatter. All of these proposed high-precision experiments may require antihydrogen atoms trapped in magnetic-multipole traps and laser-cooled to temperatures in the mK range. Appreciable fractions of antihydrogen can be confined in such traps only if they are produced at temperatures comparable to the trap depth, i.e., roughly 0.5 K.

Using confined antiproton ($\bar{p}$) and positron (e^+) plasmas, ATHENA achieved the first production of cold antihydrogen in 2002 [3], a result that was subsequently confirmed by the ATRAP experiment using a different detection technique [4]. Observations by ATRAP on the $\bar{H}$ velocity distribution [5] and by ATHENA on the spatial distribution of antihydrogen emission [6] both suggest that using the nested-well technique [7], in which hot antiprotons are launched into a positron plasma at liquid-helium temperature or slightly above, the temperature of the produced antihydrogen is several times larger than that of the positrons. This means that the recombination rate is probably much higher than the antiproton cooling rate. Even if that were not the case, the cooled $\bar{p}$ would still be subject to the rigid rotation of the positron plasma, i.e., the antiproton temperature is defined in the corotating frame of the positron plasma. Depending on the plasma parameters, this may add a significant azimuthal component to the kinetic energy of the produced antihydrogen, which scales with the square of the $\bar{p}$'s radial amplitude.

Furthermore, with a view to maximizing the lifetime of an e^+ plasma in a magnetic-multipole trap, such as those required for the capture of neutral $\bar{H}$, a plasma with a rather smaller radius than those currently used may be necessary. In order to still guarantee a good radial overlap of the antiprotons with the plasma, and to ensure the stability of the anti-

*Author to whom all correspondence should be addressed. Electronic address: a.kellerbauer@cern.ch

proton cloud itself, it may be necessary to center the $\bar{p}$ before combining them with the positrons.

Recently, an alternative scheme for $\bar{H}$ production has been demonstrated [8]. It uses multiple resonant charge exchange processes to create antihydrogen in a well-defined quantum state [9]. Since the antiprotons are not moved to a different trap region after cooling, the $\bar{H}$ are produced essentially at the temperature of the $\bar{p}$ prior to recombination. In this way, assuming sufficient care was taken not to reheat the antiprotons while ejecting the electrons that were used to cool them, antihydrogen can be produced at the temperature of the surrounding trap (though this has not yet been experimentally verified). Unfortunately, this method only allows the production of very few atoms of antihydrogen, compared with many millions created to date using the nested-well technique.

Ions in a Penning trap can be cooled by introducing a dissipative mechanism that removes energy from the motion [10]. The first realization of this technique made use of a tuned circuit to damp the signal induced in the trap electrodes by an electron's axial motion [11]. This scheme was not applicable to heavy ions, however, due to the much weaker signal induced by their slower motions, a limitation that was overcome with the introduction of a neutral buffer gas as the cooling medium [12]. This so-called sideband cooling technique is widely used today for the cooling and mass separation of collections of heavy ions in dilute neutral buffer gases.

For the cooling of hadronic antiparticles, no neutral gases are available that would not rapidly lead to the annihilation of the stored ions. We have therefore undertaken a study whose aim it was to extend this established cooling technique to non-neutral buffer gases. In this paper, we report on measurements performed with the ATHENA experiment at CERN, with a view to using this technique for the cooling and centering of antiprotons prior to recombination. Antihydrogen formed from such precentered antiprotons will be produced at or near the temperature of the surrounding trap.

II. PRINCIPLE

A. Motion of ions in an ideal Penning trap

An ideal Penning trap is achieved by superimposing a homogeneous magnetic field of magnitude B, oriented along the z axis,

$$\mathbf{B} = B\hat{z} \tag{1}$$

and a three-dimensional electrostatic quadrupolar potential,

$$\Phi = U_0 \frac{2z^2 - r^2}{2z_0^2 + r_0^2}, \tag{2}$$

where z_0 and r_0 are the characteristic dimensions of the trap and U_0 is the applied potential difference. The motion of an ion with mass m in this combined potential is described by a set of differential equations [1] which have the solutions

$$z = A_z \cos(\omega_z t - \phi_z) \quad \text{and} \tag{3a}$$

$$\mathbf{r} = R_- \begin{bmatrix} \cos(\omega_- t - \phi_-) \\ -\sin(\omega_- t - \phi_-) \end{bmatrix} + R_+ \begin{bmatrix} \cos(\omega_+ t - \phi_+) \\ -\sin(\omega_+ t - \phi_+) \end{bmatrix}, \tag{3b}$$

with

$$\omega_\pm = \frac{1}{2}(\omega_c \pm \sqrt{\omega_c^2 - 2\omega_z^2}), \tag{4}$$

where $\omega_z = \sqrt{4qU_0/[m(2z_0^2 + r_0^2)]}$ is the axial frequency, $\omega_c = qB/m$ is the cyclotron frequency of an ion in a purely magnetic field, and $R_\pm$, $\omega_\pm$, and $\phi_\pm$ are the amplitudes, frequencies, and phases of the so-called modified cyclotron motion and the magnetron motion, respectively.

A charged particle confined in a Penning trap thus performs the superposition of three simple harmonic motions, an axial mode and two radial modes. In most Penning traps devised for precision experiments, the magnetic field is of the order of several tesla while the electrostatic potentials rarely exceed a few volts. Under these circumstances, the following hierarchy in the frequencies is observed:

$$\omega_+ \gg \omega_z \gg \omega_- \tag{5}$$

and the frequency of the modified cyclotron motion can thus be several orders of magnitude larger than that of the magnetron motion. In an axially harmonic potential, an important relationship between the ion motions is that the sum of the frequencies of the radial modes is exactly the true cyclotron frequency,

$$\omega_+ + \omega_- = \omega_c. \tag{6}$$

For a further treatment of the azimuthal ion motion, the radial equation of motion is most conveniently expressed in a coordinate system spanned by two canonical vectors $\mathbf{V}^\pm$, given by

$$\mathbf{V}^\pm = \dot{\mathbf{r}} - \omega_\mp \mathbf{r} \times \hat{z} \tag{7}$$

with the inverse transformation

$$\mathbf{r} = -\frac{1}{\omega_+ - \omega_-}(\mathbf{V}^+ - \mathbf{V}^-) \times \hat{z}. \tag{8}$$

This leads to the coupled equations of motion

$$\dot{\mathbf{V}}^\pm = \omega_\pm \mathbf{V}^\pm \times \hat{z} \tag{9}$$

with the solutions

$$\mathbf{V}^\pm = A^\pm \begin{bmatrix} \cos(\omega_\pm t - \phi_\pm) \\ -\sin(\omega_\pm t - \phi_\pm) \end{bmatrix}, \tag{10}$$

where the $A^\pm$ are amplitudes that depend on the initial conditions and which are related to the radial amplitudes by

$$R_\pm = \frac{A^\pm}{\omega_+ - \omega_-}. \tag{11}$$

B. Quadrupolar excitation of the azimuthal ion motion

The radial motions of confined ions can be excited with external oscillating electric fields. The type of excitation that

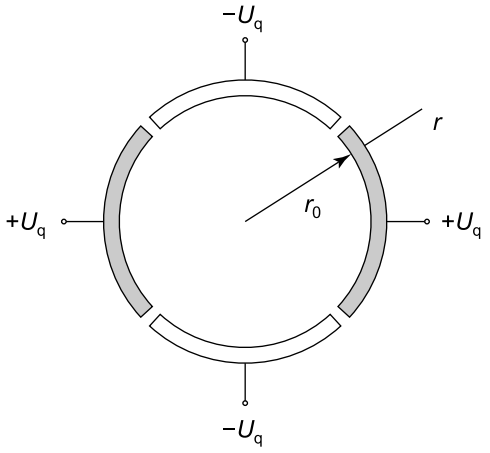

FIG. 1. Electrode geometry for the application of a quadrupolar radiofrequency potential. The figure shows an azimuthal cut through the ring electrode of a Penning trap, which is fourfold segmented to allow a quadrupolar excitation. When the potential is applied between the two pairs of opposing segments, the resulting potential has approximately a quadrupolar shape.

is of significance for cooling techniques is that performed with an azimuthal quadrupolar field. Figure 1 shows how a ring electrode is split in order to conveniently create the potentials that lead to such oscillating fields. The quadrupolar potential is of the form

$$\Phi_q = a\frac{U_q}{r_0^2}\cos(\omega_q t - \phi_q)(x^2 - y^2), \tag{12}$$

where U_q is the amplitude of the applied potential and a is a geometrical factor that takes into account the shape of the ring electrode in the azimuthal plane. In the following, only the resonant case with $\omega_q = \omega_c$ will be considered.

The additional force on the confined particles due to this quadrupolar potential leads to the following modified equations of motion:

$$\dot{\mathbf{V}}^{\pm} = \omega_{\pm}\begin{bmatrix} V_y^{\pm} \\ -V_x^{\pm} \end{bmatrix} + k_0\cos(\omega_q t - \phi_q)\begin{bmatrix} V_y^{+} - V_y^{-} \\ V_x^{+} - V_x^{-} \end{bmatrix}, \tag{13}$$

where

$$k_0 = 2a\frac{qU_q}{mr_0^2}\frac{1}{\omega_+ - \omega_-}. \tag{14}$$

These can be solved with an ansatz analogous to Eq. (10), but where the amplitudes $A^{\pm}(t)$ are now allowed to vary with time [13].

Neglecting high-frequency modulations of $A^{\pm}(t)$ and furthermore assuming that the amplitudes only change slowly and the radial motions thus remain circular, one obtains a differential equation for the canonical amplitudes,

$$\dot{A}^{\pm} = \mp\frac{1}{2}k_0 A^{\mp} e^{\pm i\Delta\phi} \tag{15}$$

with $\Delta\phi = \phi_q - \phi_+ - \phi_-$, which can be solved to yield the radial amplitudes,

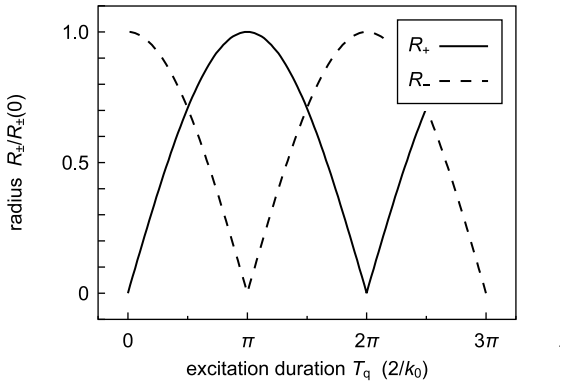

FIG. 2. Evolution of the radial amplitudes $R_{\pm}$ for $\Delta\phi = 0$ and $R_+(0) = 0$, as a function of the duration of the quadrupolar excitation T_q.

$$R_{\pm}(t) = \left| R_{\pm}(0)\cos\left(\frac{k_0}{4}t\right) \mp R_{\mp}(0)e^{\pm i\Delta\phi}\sin\left(\frac{k_0}{4}t\right)\right|. \tag{16}$$

The quadrupolar excitation thus leads to a coupling of the magnetron and modified-cyclotron motions. In a way similar to a system of coupled pendula, the motions are continually converted into each other with a conversion frequency $\omega_B = \pi k_0/2$. This process is shown in Fig. 2 for $\Delta\phi = 0$ and $R_+(0) = 0$. The degree of conversion is proportional to the amplitude U_q of the applied field and the duration T_q of the excitation. Their product is called the coupling strength of the quadrupolar excitation. In analogy with Rabi oscillations between the states of a two-level atomic system, the excitation that leads to a full conversion from one motion to another is called a π pulse.

C. Damping and cooling

1. Frictional damping

Ions lose kinetic energy in collisions with neutral atoms that have either been deliberately introduced into the trap or that remain as residual gas even under ultrahigh-vacuum conditions. The average force exerted on the particle can be approximated by a viscous-damping force,

$$\mathbf{F}_v = -\delta\dot{\mathbf{r}}, \tag{17}$$

where δ is a constant damping coefficient [14] which depends on the ion species and the buffer gas used [15,16].

The modified equation of motion under the influence of this friction force becomes

$$\dot{\mathbf{V}}^{\pm} = \omega_{\pm}\begin{bmatrix} -V_y^{\pm} \\ V_x^{\pm} \end{bmatrix} - \frac{\delta}{m}\frac{1}{\omega_+ - \omega_-}\begin{bmatrix} \omega_+ V_x^{+} - \omega_- V_x^{-} \\ \omega_+ V_y^{+} - \omega_- V_y^{-} \end{bmatrix}. \tag{18}$$

Using the ansatz and approximation already discussed above, one obtains the canonical amplitudes

$$\dot{A}^{\pm} = \alpha_{\pm}A^{\pm} \tag{19}$$

with

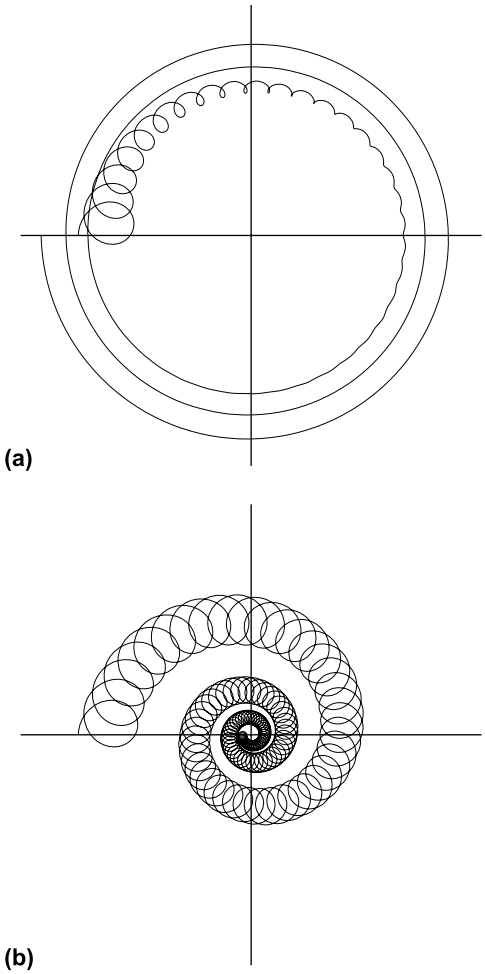

FIG. 3. Azimuthal projection of the trajectory of an ion in a buffer-gas-filled Penning trap. The hard-ball collisions between ions and buffer gas atoms are approximated by a viscous-drag force. (a) Without excitation, the cyclotron radius decreases, whereas the magnetron radius increases with a longer time constant. (b) Resonant quadrupolar excitation at the true cyclotron frequency leads to a continuous conversion of magnetron motion into cyclotron motion. The radii of both modes are decreased and the ion is centered.

$$\alpha_{\pm} = \mp \frac{\delta}{m} \frac{\omega_{\pm}}{\omega_{+} - \omega_{-}}. \tag{20}$$

and the radial amplitudes

$$R_{\pm}(t) = R_{\pm}(0) e^{\alpha_{\pm} t}. \tag{21}$$

While the modified cyclotron motion diminishes, the amplitude of the magnetron motion slowly increases until the ions eventually hit the trap electrodes and are lost. The effect of frictional damping on the radial motions is illustrated in Fig. 3(a). In typical trap configurations in which Eq. (5) holds, the time constants of the change in amplitudes are $\tau_{+} = 1/\alpha_{+} \approx m/\delta$ and $\tau_{-} = 1/\alpha_{-} \approx (m/\delta)(\omega_{+}/\omega_{-})$. The cyclotron centering is thus a much faster process than the magnetron expansion. According to Eq. (21), the modified cyclotron amplitude is reduced to zero after a sufficiently long cooling time. In a real system, however, in which the cooling is provided by a buffer gas with a finite temperature of its own, the final cyclotron radius will be $R_{+,\mathrm{th}} \approx v_{\mathrm{th}}/\omega_{+}$, where v_{th} is the thermal velocity of the ion at the temperature of the buffer gas.

2. Sideband cooling

The sideband cooling technique [12] is based on the realization that the two effects expressed in Eqs. (16) and (21) can be combined. The coupling of the two radial motions by a quadrupolar excitation at the true cyclotron frequency ω_c circumvents the problem of an increased magnetron radius in the presence of damping. As shown in Fig. 3(b), this technique allows the cooling of both radial motions. It is routinely used in beam preparation traps of experiments in which clean samples of radioactive ions are required for high-precision measurements, such as ISOLTRAP [17] at CERN/ISOLDE, which pioneered the technique. The buffer gases of choice are mainly hydrogen, helium, and nitrogen at pressures from 10^{-2} to 10^{-4} Pa.

D. Non-neutral buffer gas

In principle, the damping of an ion's radial motions can be achieved with charged particles instead of neutral buffer gas atoms. While the presence of a non-neutral plasma in the trap strongly modifies the confining electrostatic potential as seen by the ions, it is important to note that in the case of a uniform-density buffer gas plasma, the radial electric field *inside* the plasma is proportional to the radius and thus the quadrupolar shape of the overall potential is retained. The motion of the ions in the combined potential is thus formally identical to that in the unperturbed Penning trap. While the oscillation frequencies of the ions are modified, the important relation of Eq. (6) continues to hold.

The fact that the buffer gas particles are charged leads to the following important differences and their respective implications.

(i) The excitation of the motion of the ions by an external oscillating field is hampered by the space charge of the charged buffer gas. In order for the exciting field to penetrate the buffer gas plasma, its plasma frequency ω_p must be smaller than the excitation frequency ω_{exc}. This places a severe restriction on the buffer gas density, which in the case of our setup corresponds to an upper limit of about 2.6×10^7 cm^{-3}.

(ii) The collisions between the ions and the buffer gas are not hard-ball collisions, as approximated in the case of a neutral collision partner, but Coulomb interactions with infinite range. The damping coefficient of the dissipative force acting upon the ions is no longer constant but now depends on the ions' velocity [18],

$$\delta_{\mathrm{nn}} = -\frac{m\langle \Delta v_{\|} \rangle}{v_{\|}}, \tag{22}$$

where $v_{\|}$ is the instantaneous velocity of the ion and $\langle \Delta v_{\|} \rangle$ is the coefficient of dynamical friction, itself a complicated function of $v_{\|}$. If $v_{\|}$ is much larger than the root-mean-square velocity of the buffer gas particles, the coefficient behaves as

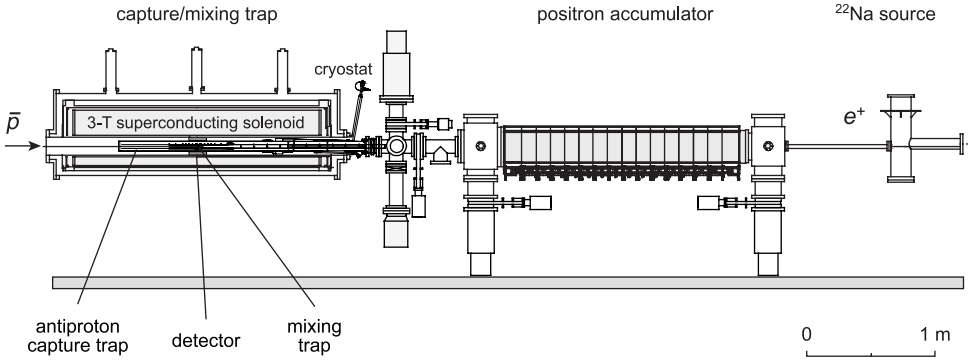

FIG. 4. Overview of the ATHENA apparatus. Shown on the left is the superconducting 3-T solenoid magnet which houses the capture trap, the mixing trap, and the antihydrogen annihilation detector. On the right, the radioactive sodium source for the positron production and the 0.14-T positron accumulation Penning trap.

$\delta_{nn} \propto v_{\|}^{-3}$. The equation that describes the radial amplitudes [Eq. (21)] can be adapted to the new situation by allowing for a varying cooling rate $\alpha_{\pm}(t)$ and time "constant" $\tau_{\pm}(t)$. The evolution of the particle trajectories under the influence of a friction force with a variable damping coefficient as given by Eq. (22) cannot be solved analytically. Nevertheless, aside from an increase in damping at reduced ion velocities, it is obvious that the overall qualitative behavior shown in Fig. 3(b) is retained.

(iii) The overall time required for the centering of a collection of ions is limited by the larger of the two time constants for conversion and cooling. When using a neutral buffer gas, one can easily adjust its pressure in order to achieve sufficiently fast cooling. In the case of a charged buffer gas, the density of the charged buffer gas is limited by the plasma frequency condition given above, and the cooling time constant will be correspondingly long. Therefore, the excitation amplitude must either be kept small or the excitation must be stopped after one full π pulse. In the latter case, since the cooling transfers part of the radial energy back to magnetron motion, the excitation must probably be applied repeatedly, leaving ample time for cooling between successive excitations.

These considerations show that buffer gas cooling with a non-neutral buffer gas should be possible, but that unlike in the neutral case the plasma density and excitation amplitude are strongly correlated and cannot be chosen independently.

III. SETUP

The ATHENA apparatus [19] consists of three main components, shown in Fig. 4: The antiproton ($\bar{p}$) capture trap, the mixing trap, and the positron (e^+) source and accumulator. The former two are located in the 3-T field of a superconducting magnet whose bore is kept at liquid-nitrogen temperature. A liquid-helium cryostat, whose cold nose protrudes into the magnet bore and encloses the trap, reduces the temperature of the trap region further to about 15 K.

The bunch of about $(2-3)\times 10^7$ antiprotons that is extracted from the Antiproton Decelerator (AD) every 80–100 s undergoes a final deceleration step in a thin ($\approx$50 μm) aluminum degrader foil, and about 10^4 $\bar{p}$ are trapped by high-voltage electrodes in the capture trap, a cylindrical Penning trap whose electrodes have an inner diameter of 25 mm. After the independent $\bar{p}$ stacking and e^+ accumulation phases, the positron plasma and the antiproton bunch are transferred to the mixing trap, where they are brought into overlap and antihydrogen production takes place.

The measurements reported here were performed in the capture trap, whose geometry is shown in Fig. 5(a). Variable dc potentials can be applied to the electrode segments, thereby allowing the creation of axial potential wells for the confinement of charged particles.

In preparation for antiproton capture, electrons are preloaded into the capture trap from an electron source mounted on a support about 2 m downstream into a very broad potential well with a small local maximum at the ring electrode. The BaO disk cathode of the electron gun produces a steady current of electrons of up to 10 μA. Typically during the operation of the electron gun, the electrodes CMP3LA or CMP3LB (see the electrode labels in Fig. 5) are kept at a negative voltage in order to reflect the beam back toward the source. Over a loading time of several seconds, a small portion of the produced electrons is trapped in a narrow well in the center of the capture trap. By choosing different trapping electrodes and potential shapes, electron clouds with different characteristics can be loaded.

Plasmas containing about 3×10^8 electrons at a density of about 10^8 cm^{-3} are thus prepared in a harmonic well centered at the ring electrode [Fig. 5(b)]. The plasma parameters length l, density n, and aspect ratio α, as well as the change in its temperature ΔT, can be determined using ATHENA's plasma diagnostics system [20] by measuring the frequencies of the first two axial plasma modes. After the capture and cooling of the antiprotons, some or all of the electrons can be ejected from the potential well by applying short electric pulses (about 100 ns duration) to electrode CMP3LA. The antiprotons with their 2000 times higher mass are practically unaffected by the electron ejection pulses. After these manipulations, the only $\bar{p}$ left in the capture trap are those which initially had radial overlap with the electron plasma.

Since electrode CMP1L was the only fourfold split electrode in the capture trap, the antiprotons (along with the remaining electrons, in the case of cooling measurements) had to be moved to the location of that electrode. For this purpose, the trap potentials for trapping as shown in Fig. 5(b) were adiabatically changed to the values displayed in Fig. 5(c), with a small square 25-V well at CMP1L. That configuration was maintained also during the excitation of the radial

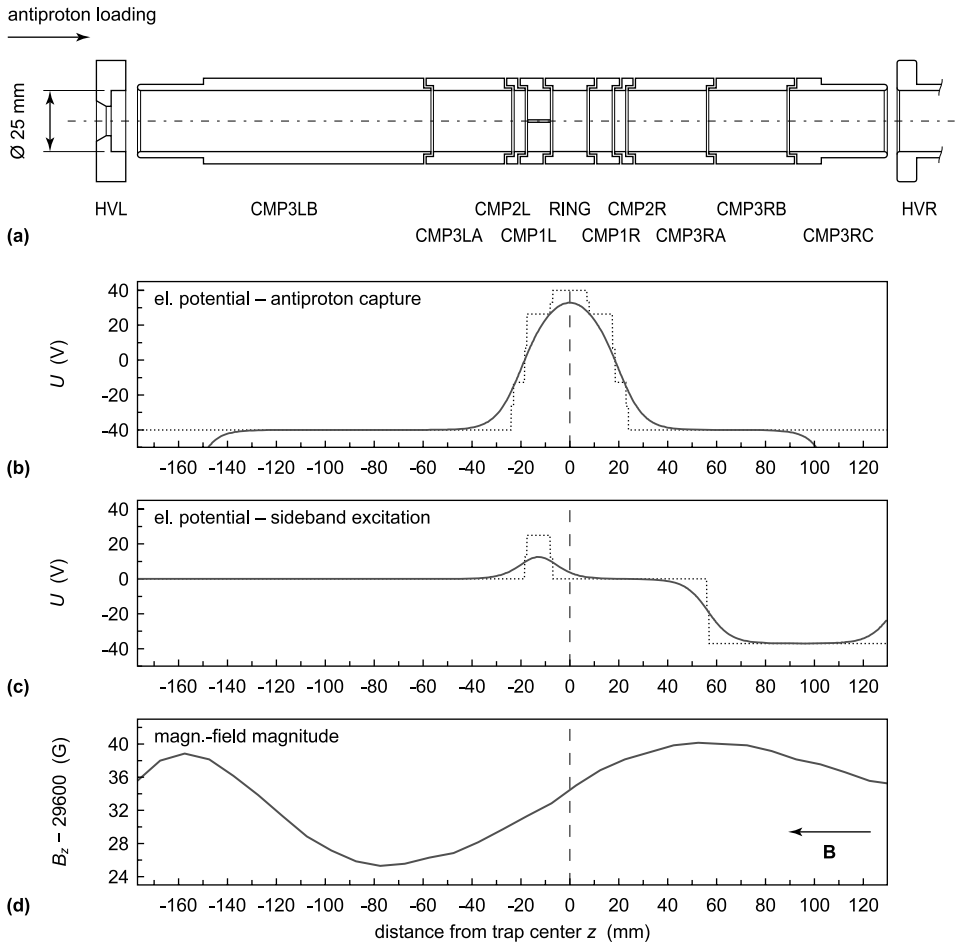

FIG. 5. (a) Geometry of the antiproton capture trap, as it was in operation in 2003. The CMP1L electrode is split fourfold to allow azimuthal quadrupolar excitation. (b) Axial electric dc trap potential for antiproton capture. (c) Axial electric dc trap potential during sideband excitation. The dotted and solid lines show the potentials at the electrodes and on the trap axis, respectively. (d) Magnetic-field magnitude on the trap axis, measured with a Hall probe. (Note the scale—the relative difference between the local minimum and maximum of the magnetic-field magnitude in this trap region is only about 5×10^{-4}.)

motions. Away from the trap axis, this applied square potential leads to an anharmonic potential and thus to a modified magnetron frequency and a deviation from the equality expressed in Eq. (6). This means that a signal at the cyclotron frequency cannot excite all particles confined in the square well, but only those for which the relation $\omega_{\mathrm{exc}}=\omega_-'+\omega_+$ holds within the bandwidth defined by the excitation duration.

In order to carefully control the duration T_q, the amplitude U_q, and the frequency ω_{exc} of the quadrupolar excitation, a digital signal processor (DSP) was used for the signal generation. The DSP (Analog Devices ADSP-2191) interfaces with a numerically controlled oscillator, which is programmable with a serial word of 32 bits, thereby allowing a frequency resolution of 1 Hz. The DSP output is then fed into an active power splitter that delivers two pairs of symmetric signals with equal amplitude and opposite phase, as required for quadrupolar excitation. The maximal duration of the programmed waveform depends on the firmware code, but was $T_{q,\mathrm{max}}=2.55$ ms for most of the measurements reported here. With the amplifier setup as described above, the maximal DSP output amplitude of 200 mV corresponded to an amplifier/splitter output of up to 2.6 V (both into a 50-Ω load). While it was not possible to measure directly the actual signal applied to the electrodes, we estimate that the attenuation due to the 2-m-long coaxial cable (Lakeshore, type SS) with stainless-steel conductor and braided stainless-steel shield is about a factor of 2. In the following, the measured amplitudes as applied to the electrical vacuum feedthrough are given.

IV. MEASUREMENTS AND RESULTS

For the measurements described in this section, antiprotons were captured and cooled in the capture trap filled with about $(2-3)\times10^8$ electrons. After a cooling phase of several seconds, all or most of the electrons were removed from the trap, thus retaining the cooled antiprotons with a very small cyclotron amplitude of a few μm but finite magnetron radii.

A. Signal for the conversion of radial motions

As discussed earlier, a quadrupolar excitation at the cyclotron frequency can convert the magnetron motion of all or some of the antiprotons to cyclotron motion. Note that even though the cyclotron frequency, and thus the kinetic energy of that motion, are much larger than in the case of the magnetron motion, the final cyclotron radius is at most as large as the initial magnetron radius. Quadrupolar excitation at the cyclotron frequency can therefore not lead to a radial loss of particles that have been successfully captured and sympathetically cooled.

Contrary to this expectation, a "loss," i.e., a shortfall of antiprotons counted in the trap dumps (toward the HVL elec-

trode) after the end of the excitation cycle was observed. No antiproton annihilations were recorded during or after sideband excitation. This observation can be explained with the concurrence of two effects. First, the excited antiprotons have a large orbital magnetic moment associated with the cyclotron motion,

$$\boldsymbol{\mu} = \frac{1}{2} e \boldsymbol{\omega}_+ R_+^2. \tag{23}$$

Second, measurements with a Hall probe have shown that ATHENA's superconducting magnet exhibits small local inhomogeneities of the magnetic field which can reach relative magnitudes of about 5×10^{-4} over the extent of the capture trap. The magnetic-field magnitude in the trap region is shown in Fig. 5(d). The magnetic-field gradient exerts a force on the magnetic moments of the ions and pulls them toward the positive z direction (toward the HVR electrode).

According to Eq. (23), the magnitude of the force scales with the square of the cyclotron amplitude at the time of the dump, which in turn is equal to the initial magnetron amplitude. It can reach about 25 eV m^{-1} near the trap center for ions with $R_+ \approx 3$ mm, high enough to prevent ejection of such antiprotons from the trap. We will present experimental evidence for this hypothesis below. In the following, a shortfall of antiprotons in the final dump is interpreted as an excitation at the true cyclotron frequency and conversion of magnetron motion to cyclotron motion.

B. Sideband excitation of antiprotons in vacuum

The absolute magnitude of the magnetic field in the capture and mixing trap region is known from the Hall probe measurements mentioned above to better than 10^{-3}. For excitation durations of several ms, however, the frequency bandwidth is less than 500 Hz, leading to a resolving power of roughly 10^5 for the cyclotron frequency of antiprotons (about 45 MHz). It was therefore necessary to initially determine the exact cyclotron frequency. For this purpose, we conducted sweeps of quadrupolar excitation pulses around the expected cyclotron frequency. As the conversion signal was observed, the sweep range was successively reduced until the frequency was found to be about 45.511 MHz. Figure 6 shows a scan, in discrete steps, of the excitation frequency. A clear disappearance signal is observed at $\omega_{\mathrm{exc}} = \omega_c$.

It is immediately obvious from Fig. 6, as well as from the other measurements described below, that only a fraction of 20–40 % of antiprotons appear to be affected by the excitation. This is due to the fact that ions with smaller initial magnetron radii are not strongly confined by the magnetic trapping effect and are therefore dumped despite successful conversion of the radial motions. The observed fraction of affected antiprotons, therefore, only constitutes a lower bound, and it is conceivable that the motions of most ions are in fact converted. Nevertheless, since the coupling frequency varies slightly with the radial position of the antiprotons, it is also possible that the excitation signal is not in resonance with all of the ions.

The coupling strength $U_q T_q$ required for two full conversions (2π), according to Eqs. (14) and (16), should be about

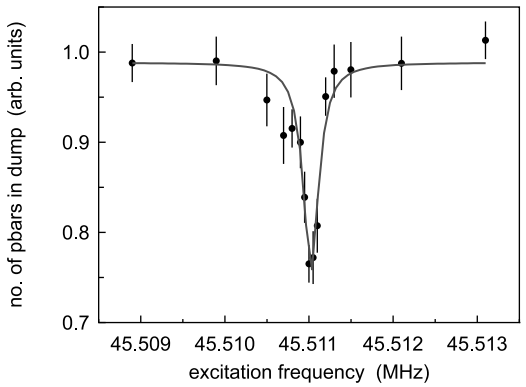

FIG. 6. Number of antiprotons observed in the dump after quadrupolar excitation. A fit to the data points (solid line) allows a determination of the cyclotron frequency. See the text for an explanation of the loss mechanism.

3.3 mV s, using a geometrical factor $a = 0.90$ as calculated numerically for our trap geometry. In order to determine its actual value and to demonstrate the conversion back from cyclotron to magnetron motion, we recorded the $\bar{p}$ disappearance as a function of the excitation amplitude for a fixed excitation duration at the cyclotron frequency. The result, shown in Fig. 7(a), is a confirmation of the resonant excitation and loss mechanism. The coupling strength required for two full conversions [second maximum of the graph in Fig. 7(a)] was found to be $U_q T_q = 2.1$ mV s. The figure also shows

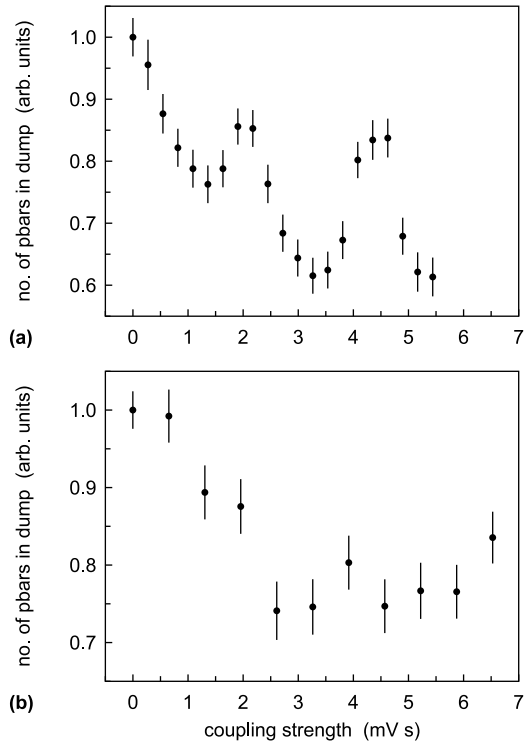

FIG. 7. Number of antiprotons observed in the dump as a function of the coupling strength $U_q T_q$ of the quadrupolar excitation. (a) Without buffer gas. (b) With electron buffer gas, number of electrons $N_{e^-} = 3 \times 10^6$.

that about 15% of the excited ions are not recovered. This effect sets in within the first two conversions and therefore appears to shift the first minimum of the graph toward higher coupling strengths.

C. Sideband excitation of antiprotons in an electron buffer gas

As the next logical step toward sideband cooling, the quadrupolar excitation was applied in the presence of electrons as a buffer medium. To this end, fewer electron kickout pulses at lower voltages were applied to electrode CMP3LA, such that between 1 and 3×10^6 electrons remained in the harmonic potential along with the antiprotons. While the density and spatial extent of the remaining electron plasma are important parameters for this technique, they could not be measured directly with the plasma mode diagnostics system due to the small number of electrons. A measurement of these quantities just before the kickout and transfer to electrode CMP1L should, however, yield an indication on the density and a lower (upper) limit of the plasma radius (length) after these manipulations. One can thus infer that the electron buffer gas plasmas used in the following had a density $n=(1-2.5)\times10^7$ cm^{-3}, a radius $r\gtrsim3$ mm, and a length $l\lesssim2.5$ mm.

Given these plasma properties, the sideband excitation frequency is higher than any of the main axial collective modes of the electron plasma [20]. Furthermore, excitation with a quadrupolar oscillating potential whose axis of symmetry coincides with the trap axis should drive neither axial nor azimuthal plasma modes (a small mechanical misalignment and a dipolar field component can of course not be ruled out). Therefore, it is expected that the excitation has no influence on the temperature of the electrons, even though a small heating effect cannot be excluded. Moreover, no loss of electrons was observed. While the full mode diagnostics system was not available, in some cases the dipole plasma mode was detectable. Tests without antiprotons confirmed that neither the amplitude nor the width of the dipole resonance changed measurably after applying the quadrupolar excitation at 45 MHz and thus confirmed that the number of electrons was unchanged. Any heating of the electron plasma that does not lead to particle loss would be compensated by cooling due to synchrotron radiation and would merely delay the sympathetic cooling by the synchrotron cooling time, which is roughly 0.4 s.

The coupling strength measurement as described in the previous section was then repeated in the presence of the electron buffer gas at the same excitation frequency. As can be seen from the resulting graph, shown in Fig. 7(b), the maximum available coupling strength was not sufficient to achieve two full π pulses, i.e., conversion back to magnetron motion. The required coupling strength can, however, be estimated to be at least three times higher than in vacuum.

The effect of the cooling and subsequent reappearance of antiprotons that have been temporarily trapped in a magnetic bottle was demonstrated by a measurement of the number of antiprotons observed in the final dump as a function of the waiting time after having applied a full π pulse. Figure 8 shows that the $\bar{p}$ which are absent from the dump if it takes

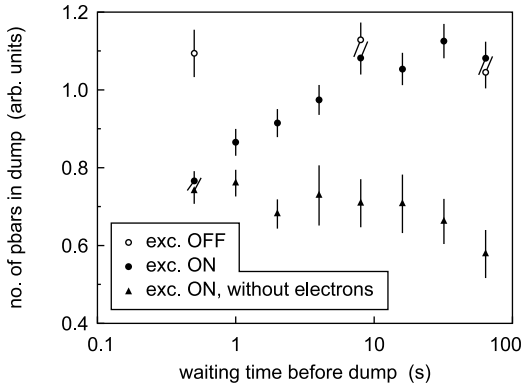

FIG. 8. Cooling of the modified cyclotron motion. Antiprotons missing from a dump immediately after the quadrupolar excitation with a π pulse are recovered after a sufficiently long waiting time after the excitation. The data points taken in the absence of electrons show that the excited antiprotons are not cooled and therefore not recovered in the dump even after waiting times of many tens of seconds.

place immediately after the excitation reappear after a sufficient waiting time. The figure confirms that the particles were not actually lost, but still present within the trap, thereby supporting our hypothesis for the disappearance mechanism. The nonlinear shape of the cooling curve on a logarithmic scale shows the variability of the cooling time "constant" due to a charged buffer gas. From the first few data points of the graph, a cooling time constant of the modified cyclotron motion of about 5 s can be inferred. Furthermore, the figure shows that in the absence of the electron buffer gas, the antiprotons whose motions have been converted are not recovered, even after very long waiting times.

This means that after at most 15 s, the cyclotron amplitudes of those antiprotons that have been resonantly excited in the presence of the electron buffer gas have returned to their initial values before the excitation, i.e., a few μm. At the same time, barring the existence of an anomalous outward radial transport during the cooling of the cyclotron motion, also the magnetron amplitudes have been considerably reduced. Assuming a complete conversion of the radial modes, the final magnetron radius should be of the same order as the cyclotron radius. An anomalous radial transport seems improbable because no antiproton loss is observed for many tens of minutes during storage with electrons. As is common in this kind of electromagnetic trap, the storage time is limited by asymmetries in the confining fields, but the time scale of transport due to asymmetries is typically much longer than the cooling time of the cyclotron motion.

At identical amplitudes, the rotational kinetic energy of ions that perform cyclotron motion is many orders of magnitude higher than that of ions that perform magnetron motion, as follows from Eq. (5). Assuming a process exists that couples the two motions in the absence of external excitation, it is therefore conceivable that a substantial amount of kinetic energy is transferred back to the magnetron mode while the cyclotron motion is being cooled. The hard-ball collisions encountered in interactions with a *neutral* buffer gas can constitute such a process, but the infinite-range Cou-

lomb interaction between the confined ions and a non-neutral buffer gas approximates the viscous force of Eq. (17) well and a coupling of the radial motions should be negligible. If such a reheating of the magnetron motion turns out to be substantial, the cyclotron cooling rate must be increased such that conversion and cooling take place simultaneously. This can be achieved by maximizing the buffer gas density within the constraints discussed in II D.

On very long time scales, centrifugal separation of the confined species can set in due to their different mass [21]. This effect will eventually push the antiprotons outside of the boundary of the electron cloud. After a sideband excitation and sufficient waiting time to allow for the cooling of the cyclotron motion, the buffer gas will therefore have to be removed from the trap. It remains to be checked whether the ejection of the electrons will disturb and reheat the cooled and centered antiprotons. This should not be the case if the kickout pulse for this operation is applied in a completely axially symmetric manner and if furthermore there is no coupling between radial and axial motions due to a deviation of the trap axis from the magnetic-field orientation.

V. CONCLUSIONS AND OUTLOOK

We have proposed a scheme for the centering of antiprotons prior to mixing with positrons for recombination. Our initial experimental investigations using the ATHENA apparatus indicate that the fourfold segmented ring electrode of a cylindrical Penning trap can be used to convert the radial motions of antiproton clouds containing several thousand particles.

By use of a unique diagnostics scheme based on the presence of magnetic-field inhomogeneities in the trap region, conversion between the radial modes has been demonstrated in vacuum. The complete mapping out of the conversion over more than one π pulse in the presence of several 10^6 electrons, however, was hampered by a lack of available coupling strength.

Lastly, the cooling of the modified cyclotron motion following a full conversion has been shown and a cooling time constant of roughly 5 s was inferred. The reappearance of previously "lost" ions supports our hypothesis for the loss mechanism and diagnostics method.

The work presented here was subject to the limitation that antiprotons supplied by the AD are scarce and have to be shared among several experiments. Nevertheless, the first results are encouraging and consistent with antiproton centering. Further studies are required in order to unambiguously demonstrate and quantify the reduction of the magnetron amplitude. If the scheme can be successfully incorporated into the antihydrogen production cycle, it will not only allow the production of $\overline{\mathrm{H}}$ as cold as the surrounding trap, but also increase the production rate due to better overlap between $\bar{p}$ and e^+, as well as improve the overlap with laser beams for stimulated recombination or laser cooling.

ACKNOWLEDGMENTS

We thank CERN, its AB Department, and the AD team for the excellent antiproton beam. This work was supported by the funding agencies CNPq (Brazil), INFN (Italy), MEXT (Japan), SNF (Switzerland), SNF (Denmark), and EPSRC (UK).

[1] L. S. Brown and G. Gabrielse, Rev. Mod. Phys. **58**, 233 (1986).
[2] J. Y. Hémery and S. Maury, Nucl. Phys. A **655**, 345c (1999).
[3] M. Amoretti *et al.*, Nature (London) **419**, 456 (2002).
[4] G. Gabrielse *et al.*, Phys. Rev. Lett. **89**, 213401 (2002).
[5] G. Gabrielse *et al.*, Phys. Rev. Lett. **93**, 073401 (2004).
[6] N. Madsen *et al.*, Phys. Rev. Lett. **94**, 033403 (2005).
[7] G. Gabrielse *et al.*, Phys. Lett. A **129**, 38 (1988).
[8] C. H. Storry *et al.*, Phys. Rev. Lett. **93**, 263401 (2004).
[9] E. A. Hessels, D. M. Homan, and M. J. Cavagnero, Phys. Rev. A **57**, 1668 (1998).
[10] D. Wineland and H. Dehmelt, Int. J. Mass Spectrom. Ion Phys. **16**, 338 (1975); **19**, 251 (1976).
[11] R. S. Van Dyck, Jr., P. B. Schwinberg, and H. G. Dehmelt, in *New Frontiers in High Energy Physics*, edited by B. Kursunoglu, A. Perlmutter, and L. F. Scott (Plenum, New York, 1978), p. 159.
[12] G. Savard *et al.*, Phys. Lett. A **158**, 247 (1991).
[13] G. Bollen *et al.*, J. Appl. Phys. **68**, 4355 (1990).
[14] E. W. McDaniel and E. A. Mason, *The Mobility and Diffusion of Ions in Gases* (Wiley, New York, 1973).
[15] H. W. Ellis *et al.*, At. Data Nucl. Data Tables **17**, 177 (1976).
[16] H. W. Ellis *et al.*, At. Data Nucl. Data Tables **22**, 179 (1978).
[17] G. Bollen *et al.*, Nucl. Instrum. Methods Phys. Res. A **368**, 675 (1996).
[18] L. Spitzer, *Physics of Fully Ionized Gases*, 2nd ed. (Wiley, New York, 1962), Chap. 5.
[19] M. Amoretti *et al.*, Nucl. Instrum. Methods Phys. Res. A **518**, 679 (2004).
[20] M. Amoretti *et al.*, Phys. Rev. Lett. **91**, 055001 (2003).
[21] T. M. O'Neil, Phys. Fluids **24**, 1447 (1981).
[22] In the following, an ion is understood to mean any charged particle, elementary or composite.